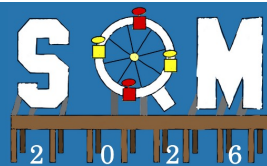




The 22<sup>nd</sup> International Conference on  
**Strangeness in Quark Matter**  
22-27 March, 2026, Los Angeles, CA



# Measurements of Local Polarization of $\Lambda$ Hyperons with Event Shape Engineering in Au+Au collisions at RHIC-STAR

Taiki Kondo (University of Tsukuba)  
for the STAR Collaboration

Supported in part by



U.S. DEPARTMENT  
of **ENERGY**

Office of  
Science



**QGP**

International Research Center  
University of Tsukuba

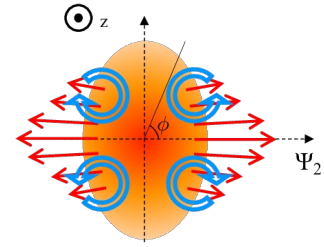


筑波大学  
*University of Tsukuba*

# Physics motivation

## Local polarization

- Anisotropic flow is expected to generate local vorticities along the beam direction.  
→ Leads to particle polarization

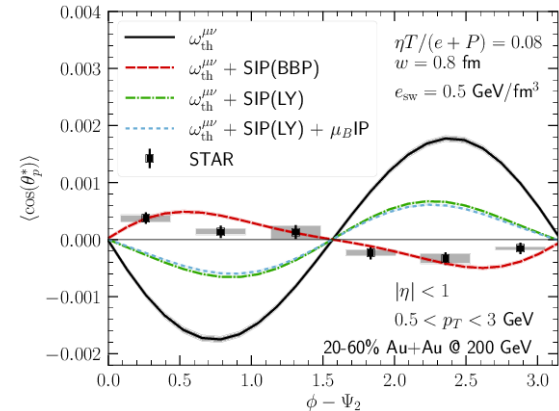


STAR, PRL131, 202301 (2023)

## Spin puzzle

- Current theoretical models cannot completely explain data observed at RHIC and the LHC.
- Some models suggest that local polarization may originate from mechanisms other than the kinematic vorticity.

Wu et al., PRR1, 033058 (2019)  
Fu et al., PRC103, 024903 (2021)

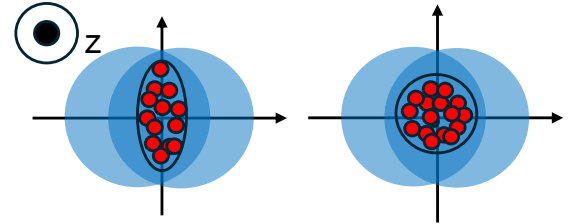


Alzhrani et al., PRC106, 014905 (2022)

# Physics motivation

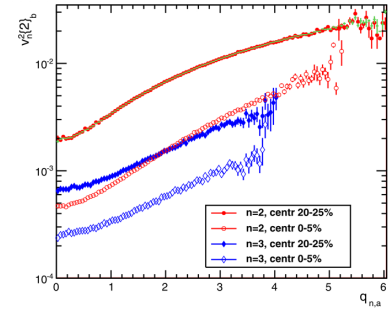
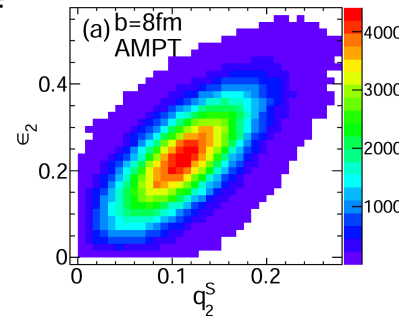
## □ Event Shape Engineering (ESE)

- A method to select events with different magnitudes of final-state flow within a narrow centrality range.
- Enables separating the difference of initial geometry.



- We measured elliptic flow and local polarization of  $\Lambda$  with ESE in  $\sqrt{s_{NN}} = 19.6$  GeV Au+Au collisions.
- Our goal is to experimentally reveal the link among the initial geometry, elliptic flow, and local polarization.

Initial eccentricity  $\epsilon_2$  or  $v_2$  vs. flow vector  $q_2$

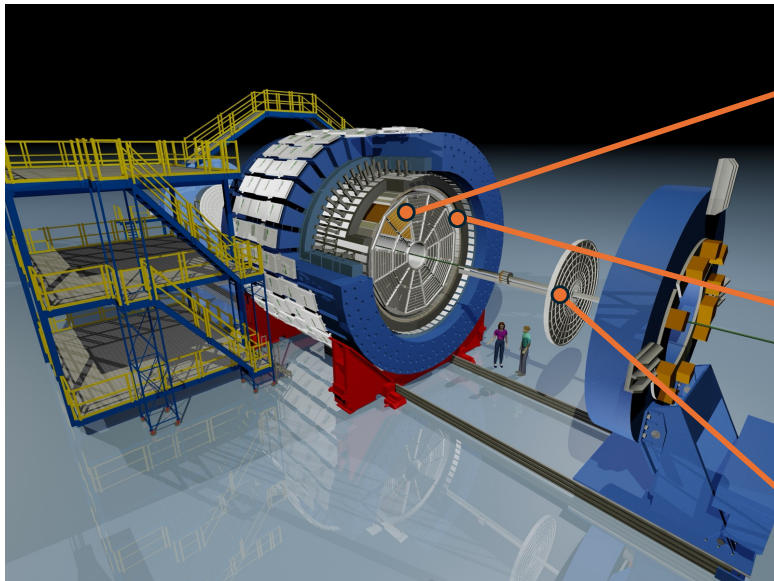


Huo et al., PRC90, 024910 (2014)

Schukraft et al., PLB719, 394 (2013)

# The STAR detector

Sub-systems mainly used in this analysis:



## Time Projection Chamber

- Reconstruction of charged-particle tracks
- PID utilizing ionization energy loss
- Wider acceptance by the iTPC upgrade ( $|\eta| < 1.5$ )

## Time of Flight Detector

- Improved PID accuracy
- $|\eta| < 0.9$

## Event Plane Detector

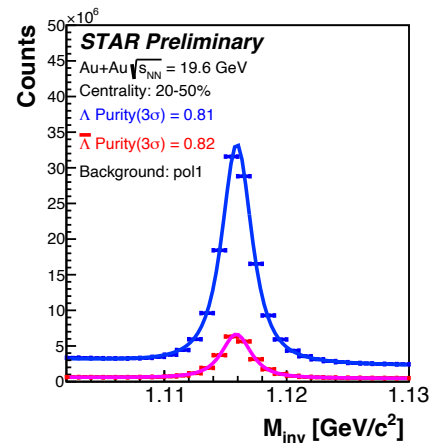
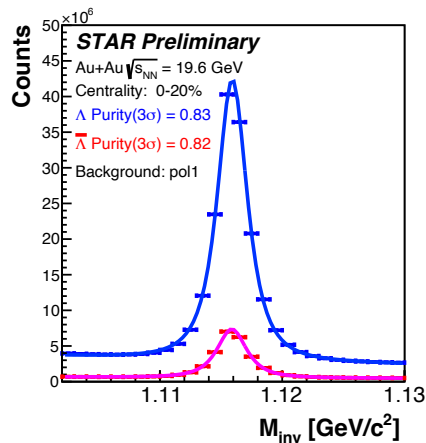
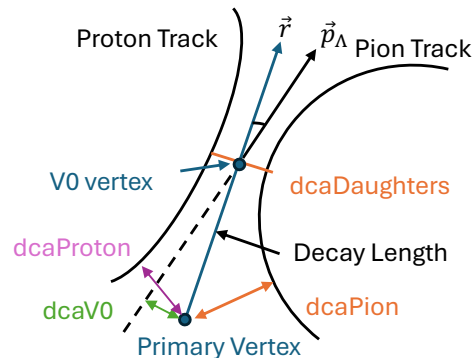
- Event plane determination
- $2.14 < |\eta| < 5.08$

# $\Lambda$ reconstruction

$$\Lambda \rightarrow p + \pi^-$$

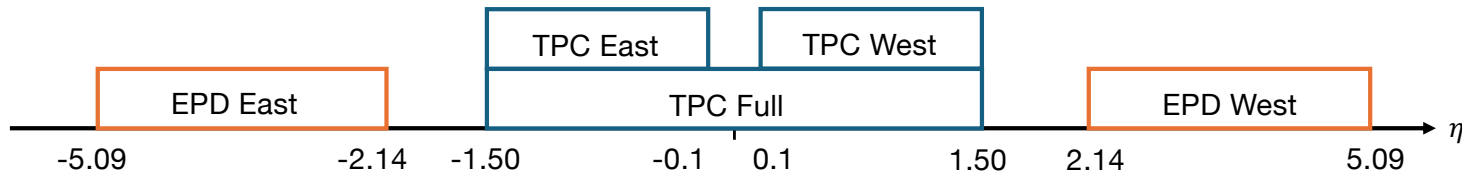
$$\bar{\Lambda} \rightarrow \bar{p} + \pi^+$$

- PID using TPC and ToF information
- $\Lambda$  reconstructed using decay topology
- Kinematic cuts for  $\Lambda$ 
  - $|\eta_\Lambda| < 1.5$
  - $0.5 < (p_\Lambda)_T < 10.0 \text{ GeV}/c$
- Fitted with Student's t-function to estimate purity
- Only daughter pairs within  $\pm 3\sigma$  around the mean were selected for further analysis.



# Event plane determination

Sub-events definition in this analysis:



- Track selection for TPC:  $0.15 < p_T < 2.0 \text{ GeV}/c$
- For EPD:  $nMip \geq 0.3$

- Q-vector

$$Q_2^x = \sum_i \omega_i \cos(2\phi_i), \quad Q_2^y = \sum_i \omega_i \sin(2\phi_i)$$

- Event plane angle

$$\Psi_2 = \frac{1}{2} \arctan\left(\frac{Q_2^y}{Q_2^x}\right) \quad \text{where } \Psi_2 \in \left[-\frac{\pi}{2}, \frac{\pi}{2}\right]$$

nMip: number of minimum ionizing particles

$\phi_i$ : azimuthal angle of charged particles

$\omega_i = p_T$  (for TPC), nMip (for EPD, if nMip > 3, used 3)

Calibration: re-centering and flattening

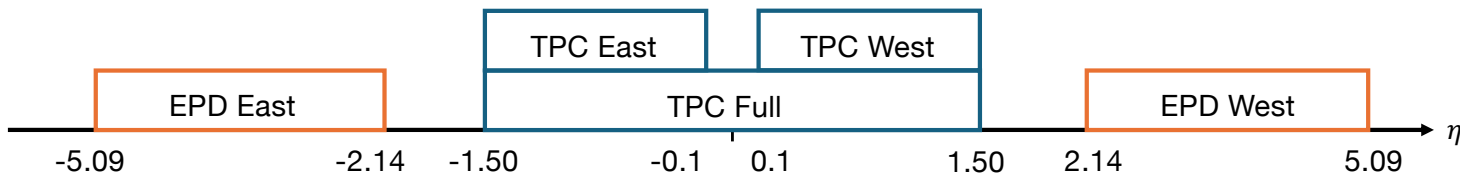
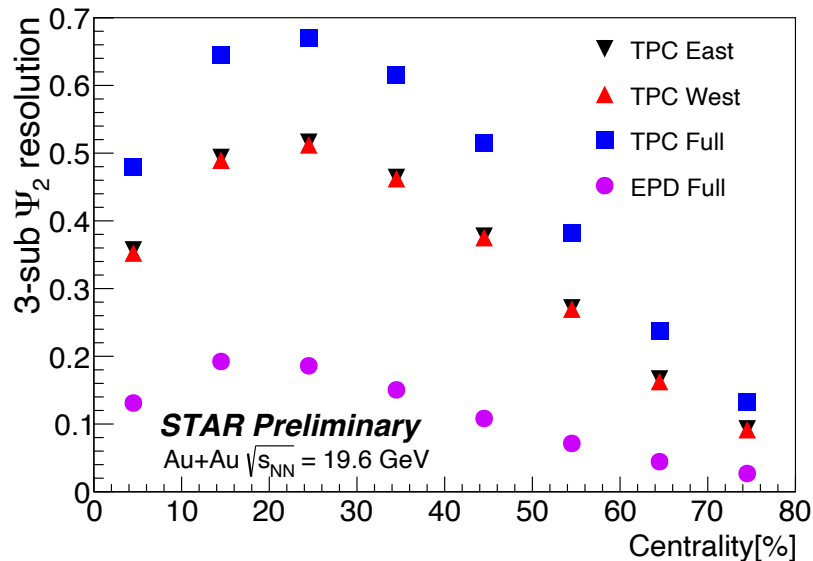
- Performed for each run number, z-vertex range (10 cm steps), and centrality range (10% steps)

# Event plane resolution

Event plane resolution by 3-sub event method:

$$Res\{\Psi_2^A\} = \sqrt{\frac{\langle \cos[2(\Psi_2^B - \Psi_2^A)] \rangle \langle \cos[2(\Psi_2^C - \Psi_2^A)] \rangle}{\langle \cos[2(\Psi_2^B - \Psi_2^C)] \rangle}}$$

A	B	C
TPC Full	EPD East	EPD West
TPC East (West)	EPD East	EPD West
EPD Full	TPC East	TPC West



# Event Shape Engineering

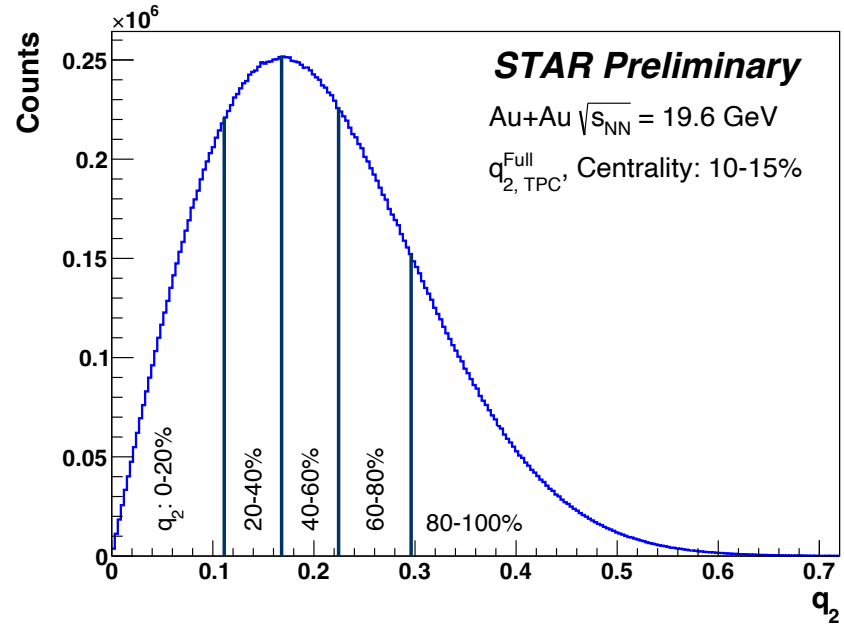
Based on  $q_2$ , events were divided into 5 classes with equal number of events (20% each)

Schukraft et al., PLB719, 394 (2013)

$$q_{2 \text{ TPC}} = \frac{|q_2|}{\sqrt{\sum p_T}}$$

To avoid multiplicity bias in event-shape selection,  $q_2$  selection was performed in narrow centrality (and multiplicity) bins:

- Centrality 10-80%: 5% steps
- For 0-5% and 5-10%: Events were further divided into 4 groups based on measured multiplicity, and then  $q_2$  selection was applied to each group.



# Measurements of $v_2$ and $P_{z,2}$ with ESE

$$v_2 = \frac{\langle \cos[2(\phi_\Lambda - \Psi_2)] \rangle}{\text{Res}\{\Psi_2\}}$$

$$P_{z,2} = \frac{1}{\alpha_\Lambda \langle \cos^2 \theta_p^* \rangle} \frac{\langle \cos \theta_p^* \sin(2(\phi_\Lambda - \Psi_2)) \rangle}{\text{Res}\{\Psi_2\}}$$

$\alpha_\Lambda$ :  $\Lambda$  decay parameter  $\alpha_\Lambda = -\alpha_{\bar{\Lambda}} = 0.747 \pm 0.010$

$\theta_p^*$ : polar angle of the daughter proton in  $\Lambda$  rest frame

$\phi_\Lambda$ : azimuthal angle of  $\Lambda$  particle

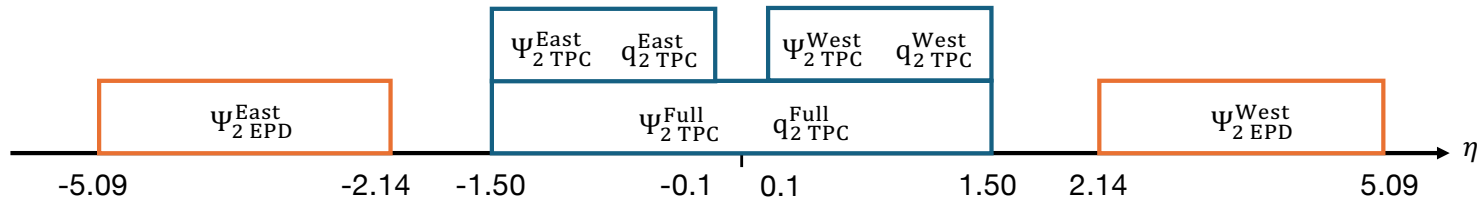
To study possible event bias,  $v_2$  and  $P_{z,2}$  of  $\Lambda$  measured with:

1.  $\Psi_{2 \text{ TPC}}^{\text{Sub}}$  and  $q_{2 \text{ TPC}}^{\text{Sub}}$  (if  $\eta_\Lambda > 0$ , used  $\Psi_{2 \text{ TPC}}^{\text{East}}$  and  $q_{2 \text{ TPC}}^{\text{East}}$ )
2.  $\Psi_{2 \text{ TPC}}^{\text{Full}}$  and  $q_{2 \text{ TPC}}^{\text{Full}}$
3.  $\Psi_{2 \text{ EPD}}^{\text{Full}}$  and  $q_{2 \text{ TPC}}^{\text{Sub}}$  (if  $\eta_\Lambda > 0$ , used  $q_{2 \text{ TPC}}^{\text{East}}$ )
4.  $\Psi_{2 \text{ EPD}}^{\text{Full}}$  and  $q_{2 \text{ TPC}}^{\text{Full}}$

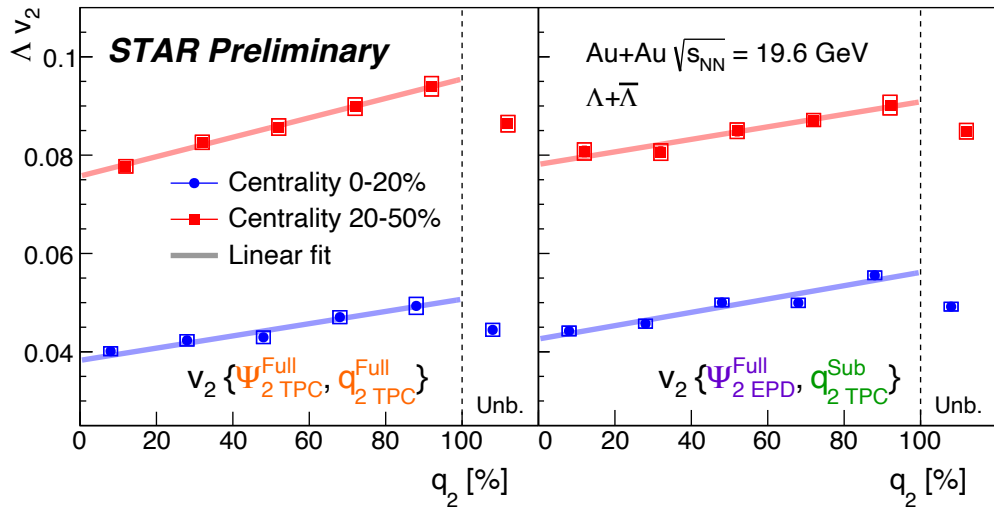
Purity correction

$$v_2^{\text{Obs}} = \text{Purity} \times v_2^{\text{Sig}} + (1 - \text{Purity}) \times v_2^{\text{Bkg}}$$

Daughter tracks were removed from  $\Psi_2$  and  $q_2$  calculations to avoid self-correlation.



# $q_2$ dependence of $v_2$

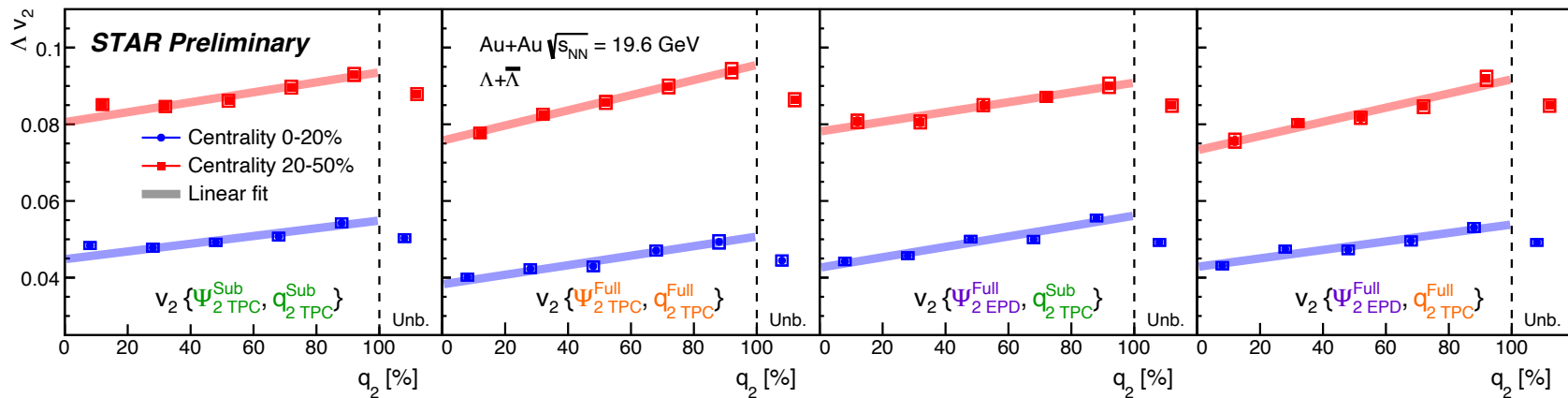


Left:  $\Psi_{2 \text{ TPC}}^{\text{Full}}$  and  $q_{2 \text{ TPC}}^{\text{Full}}$

Right:  $\Psi_{2 \text{ EPD}}^{\text{Full}}$  and  $q_{2 \text{ TPC}}^{\text{Sub}}$  (if  $\eta_{\Lambda} > 0$ , used  $q_{2 \text{ TPC}}^{\text{East}}$ )

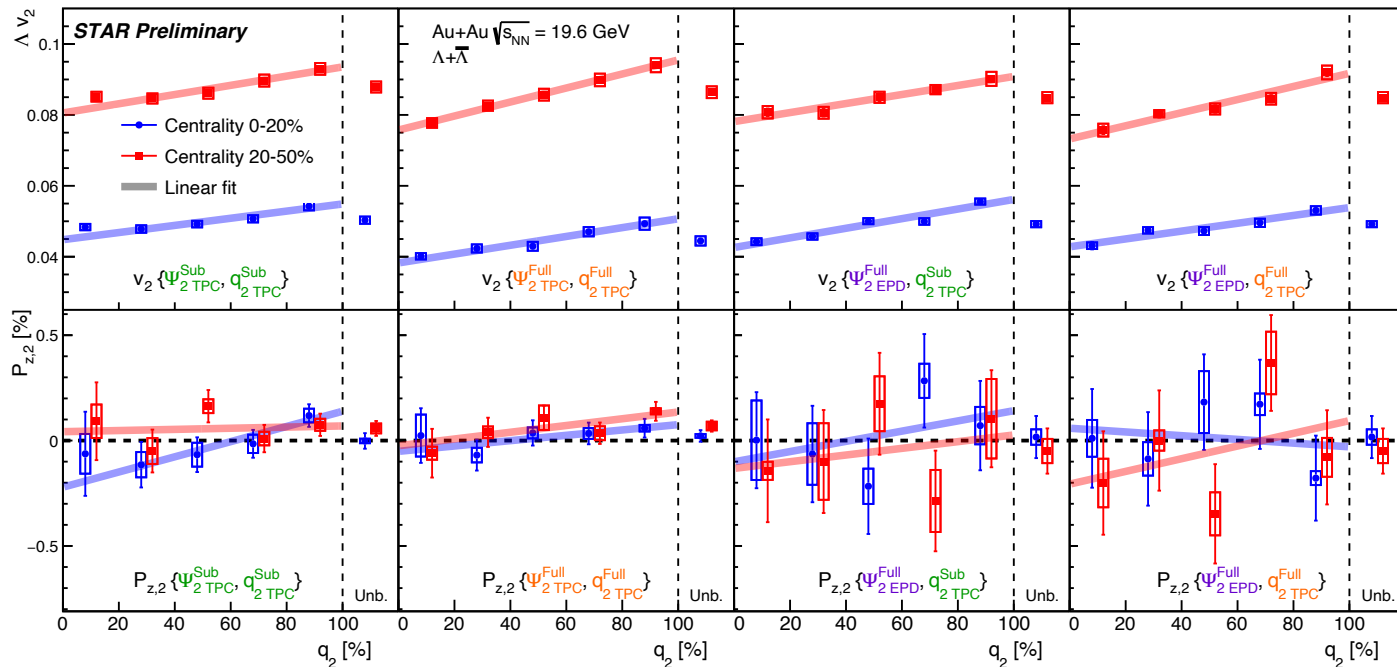
- $\Delta v_2$  changes with  $q_2$  of charged particles by about 20%.
- Specifically ( $\Psi_{2 \text{ EPD}}^{\text{Full}}, q_{2 \text{ TPC}}^{\text{Sub}}$ ) is clean combination as it uses separate  $\eta$  regions for  $\Psi_2, q_2$ , and  $v_2$ .
- The trends for 2 combinations are consistent with each other
- Note:  $q_2$  event selection and non-flow effect are different for the two cases.

# $q_2$ dependence of $v_2$



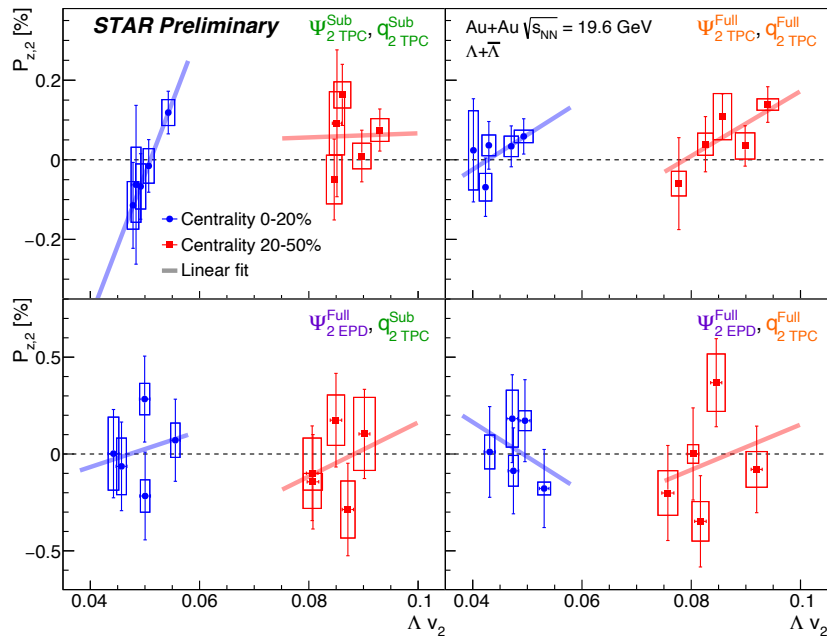
- $v_2$  shows a clear  $q_2$  dependence for all the  $(\Psi_2, q_2)$  combinations.
- The  $v_2$  results are consistent across all combinations.
- Given this consistency, the combination  $(\Psi_2^{\text{Full TPC}}, q_2^{\text{Full TPC}})$  is a better measurement owing to its highest  $\Psi_2$  resolution and  $q_2$  sensitivity.

# $q_2$ dependence of $v_2$ and $P_{z,2}$



- $P_{z,2} \{ \Psi_{2\text{TPC}}^{\text{Sub}}, q_{2\text{TPC}}^{\text{Sub}} \}$  and  $P_{z,2} \{ \Psi_{2\text{TPC}}^{\text{Full}}, q_{2\text{TPC}}^{\text{Full}} \}$  indicate a slight dependence on  $q_2$  ( $\sim 1.5\sigma$  effect).
- Measurements with EPD are obscured due to lower resolution.

# $v_2$ vs. $P_{z,2}$



- $P_{z,2}\{\Psi_{2 \text{ TPC}}^{\text{Sub}}, q_{2 \text{ TPC}}^{\text{Sub}}\}$  and  $P_{z,2}\{\Psi_{2 \text{ TPC}}^{\text{Full}}, q_{2 \text{ TPC}}^{\text{Full}}\}$  exhibit a slight dependence on  $v_2$  ( $\sim 2.0\sigma$  effect).
- Intercept seems to be negative ( $\sim 1.5\sigma$  effect).  
→ Possibly other polarization mechanisms?

# Summary

- Elliptic flow and local polarization of  $\Lambda + \bar{\Lambda}$  have been studied in Au+Au collisions at 19.6 GeV with ESE.
  - First attempt to measure the relation between  $v_2$  and  $P_{z,2}$
- $P_{z,2} \{ \Psi_{2\text{ TPC}}^{\text{Sub}}$  and  $q_{2\text{ TPC}}^{\text{Sub}} \}$  and  $P_{z,2} \{ \Psi_{2\text{ TPC}}^{\text{Full}}$  and  $q_{2\text{ TPC}}^{\text{Full}} \}$  indicate a slight dependence on  $q_2$  (charged particles) and  $v_2$  ( $\Lambda$ ).
- Outlook: measurements in 200 GeV Au+Au collisions

